

Electronic Supplementary Information

Surface Engineering of Nanoporous Silicon Photocathodes for Enhanced Photoelectrochemical Hydrogen Production

Jing-Xin Jian,^a Ming-Ming Yao,^a Jia-Xin Liao,^a Mu-Han Zhou,^a Yi-Jing Chen,^a Meng-Xin Deng,^a Xing-Yi Li,^a Jia-Ying Lin,^a Yu-Mei Huang,^a Chao-Ping Liu^b and Qing-Xiao Tong^{*,a}*

^aDepartment of Chemistry, Key Laboratory for Preparation and Application of Ordered Structural Materials of Guangdong Province and Guangdong Provincial Key Laboratory of Marine Disaster Prediction and Prevention, Shantou University, Guangdong 515063, P. R. China.

**Corresponding Author:*

J. X Jian, Email: jxjian@stu.edu.cn;

Q.-X. Tong, Email: qxtong@stu.edu.cn

^bDepartment of Physics, Shantou University, Shantou, Guangdong, 515063, P.R. China

Materials and Instruments.

The silicon wafers used in the experiment were commercial silicon wafers purchased from Zhejiang Jingyou Silicon Technology Co., Ltd, which were then used after a series of treatments. 100 μm of boron doped p-type (100) Si wafer with resistivity of 1~10 $\Omega\text{ cm}$ was used to fabricate nanoporous Si photoelectrodes during the whole experiment. Hydrofluoric acid (HF, 48.0~55.0% w/w in water) were purchased from Energy Chemical Company. Field emission scanning electron microscope (FESEM) and the related EDXS morphologies were recorded on a Zeiss Gemini 300 instrument. The reflectance spectrum of materials was measured on a Lambda 950 UV/VIS Spectrometer. All X-ray Multifunctional imaging electron spectrometer experiments were obtained on a Thermo ESCALAB 250Xi with a monochromatized Al $K\alpha$. PEC measurements were carried out on a CHI660E potentiostat. The standard AM1.5G 100 mW cm^{-2} from the solar simulator (China Education Au-Light Co., Ltd) was used as light source for PEC water splitting.

Fabrication of nanostructured Si photocathodes

Si photocathode (*f*-Si) were fabricated using flat Si wafer with ohmic contact of 200 nm Al on the backside (**Figure S1**). The Si wafer was connected to Cu tape, fixed on a plastic plate, and sealed the edges with epoxy resin. Thus, only the front surface of Si was exposed to an electrolyte and light for etching and PEC measurements. Chemical-etched Si (*c*-Si) pyramids were fabricated by applying a chemical wet etching method. The *f*-Si electrode was immersed in a 200 ml solution consisting of 4.01 g of KOH and 10 mL of isopropyl alcohol, and then heat to 90 $^{\circ}\text{C}$. Following, the chemical-etched Si electrode was rinsed with DI water and blown dry under a N_2 flow.

For the electrochemical-etching and photoelectrochemical-etching, the *f*-Si photoelectrode was used as the working electrode, the platinum sheet electrode was used as the counter electrode, and 5% hydrofluoric acid was used as the electrolyte to form a two-electrode system for the hydrofluoric acid photoanode etching. The concentration of the hydrofluoric acid electrolyte is 5%, the current is maintained at 100 mA, and the time is 2000 seconds. At the same time, while keeping the current constant, the electrode can be optimized by changing the etching time. Using planar silicon photoelectrodes under different conditions, two different types of silicon electrodes were prepared. The only difference between the *ec*-Si and *pec*-Si is that the hydrofluoric acid photoanode etching (*pec*-Si) is prepared under illumination. Violet ($400 \pm 10\text{ nm}$), blue ($450 \pm 10\text{ nm}$), green ($520 \pm 10\text{ nm}$) and red ($620 \pm 10\text{ nm}$) LEDs (3W, $\sim 50\text{ mW/cm}^2$) are used as the light

source, the optimal light source is red LED (Figure S2). The prepared Si photoelectrodes will be dried with N_2 . The TiO_2 thin film was deposited on Si photocathodes by radio frequency magnetron sputtering from the TiO_2 (99.99%) target without substrate heating. Before sputtering, the chamber was pumped down to a base pressure of 7.5×10^{-6} Torr, and the sputtering was conducted in pure Ar gas with the chamber pressure maintained at 3.7 mTorr. The thickness of TiO_2 film was controlled by the deposition power and time, which were set to 60 W and 40 minutes to prepare 100 nm TiO_2 .

Electrochemical characterizations

Electrochemical experiments were measured on a CHI660E potentiostat, in a three-electrode system consisting of the prepared Si photocathode, the counter electrode of $1 \times 1 \text{ cm}^2$ Pt plate and the reference electrode Ag/AgCl (saturated KCl) (Figure S3). The simulated sunlight of AM1.5G (100 mW cm^{-2}) was supplied from the solar simulator (China Education Au-Light Co., Ltd). Before the PEC measurements, the 0.5 M H_2SO_4 electrolyte was deoxygenated by bubbling Ar (99.9%). All J - V curves were recorded at a scan rate of 30 mV s^{-1} . The amount of the produced H_2 was detected by gas chromatograph (GC7920) with a TCD detector. The H_2 evolution Faradaic efficiency (η_{H_2}) of *pec*-Si/ TiO_2 was calculated by the ratio of the detected H_2 gas from working electrode (n_{H_2}) and the detected H_2 in an electrolysis system ($n_{H_2'}$) of two Pt electrodes with assuming H_2 evolution Faradaic efficiency of 100% ($\eta_{Pt-Pt} = 100\%$) in the same conditions. Thus, $\eta_{H_2} = n_{H_2} / n_{H_2'} \times \eta_{Pt-Pt}$.

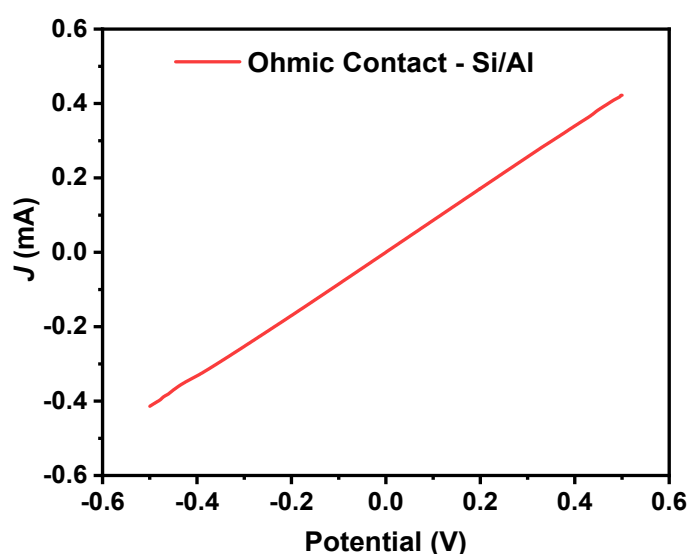


Figure S1. Current-voltage curve of 200-nm Al/Si ohmic contact on backside of Si.

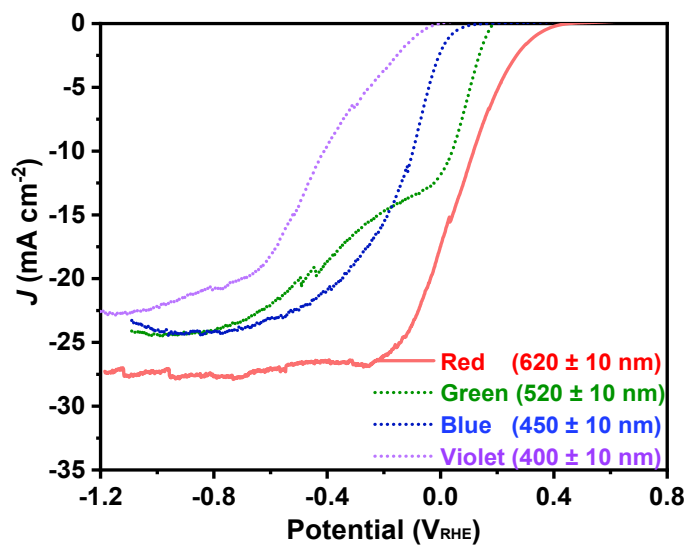


Figure S2. J - V curves of photoelectrochemical-etching Si photocathodes in 0.5 M H_2SO_4 electrolyte under AM1.5G illumination, which are fabricated using different LED light sources.

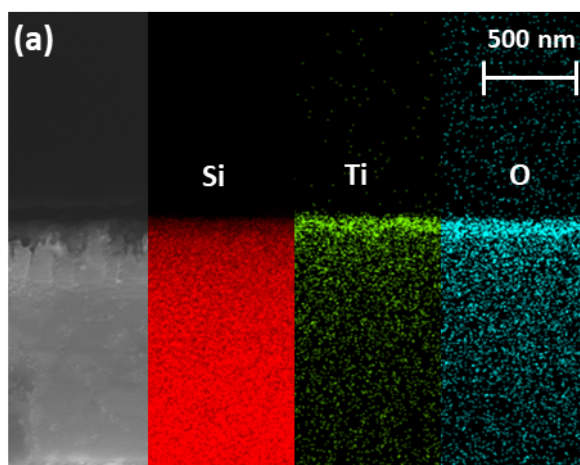


Figure S3. SEM image of *pec*-Si/TiO₂ and the related EDXS images of Si, Ti and O elements.

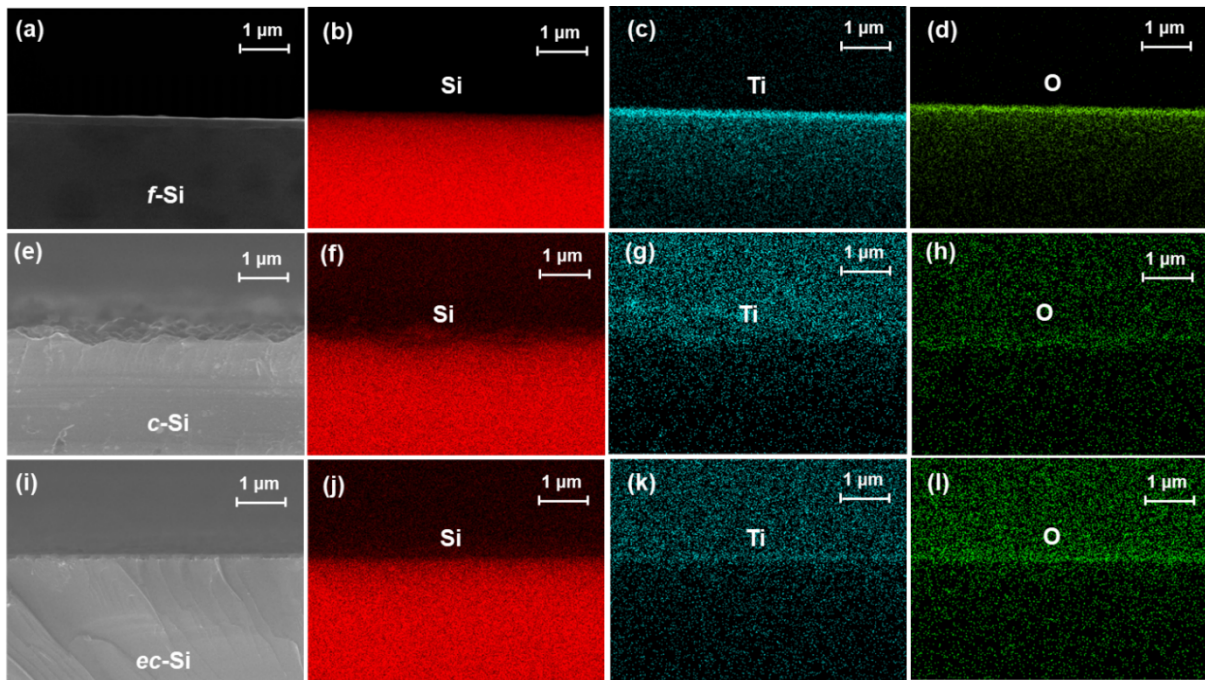


Figure S4. SEM images of *f*-Si/TiO₂, *c*-Si/TiO₂, *ec*-Si/TiO₂ and the related EDXS images of Si, Ti, O elements.

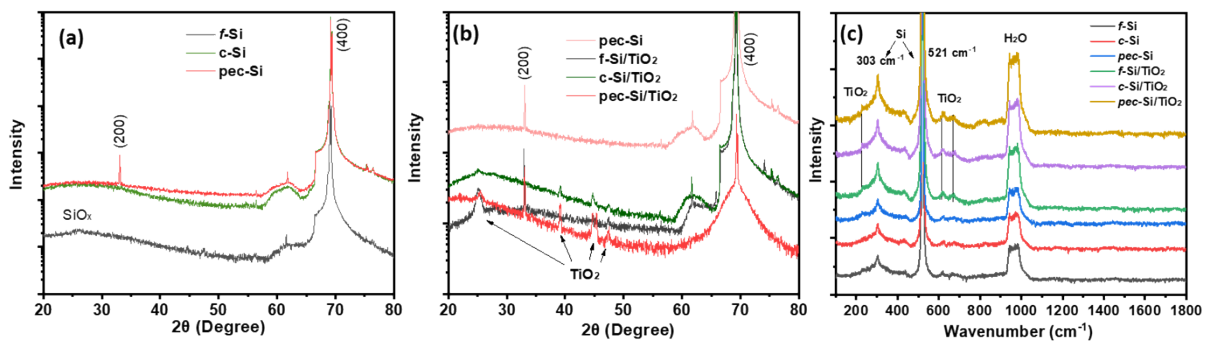


Figure S5. XRD pattern of *f*-Si, *c*-Si, and *pec*-Si before (a) and after (b) deposition of TiO₂, (c) Raman spectra of *f*-Si, *c*-Si, and *pec*-Si with and without TiO₂ layer.

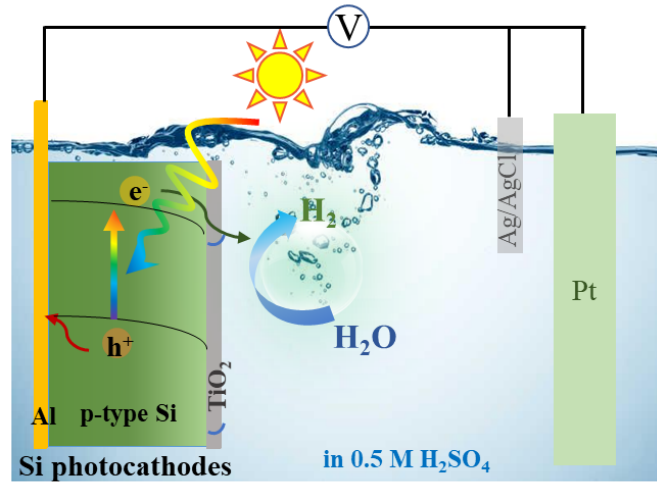


Figure S6. Configuration of PEC water splitting system by Si photocathodes.

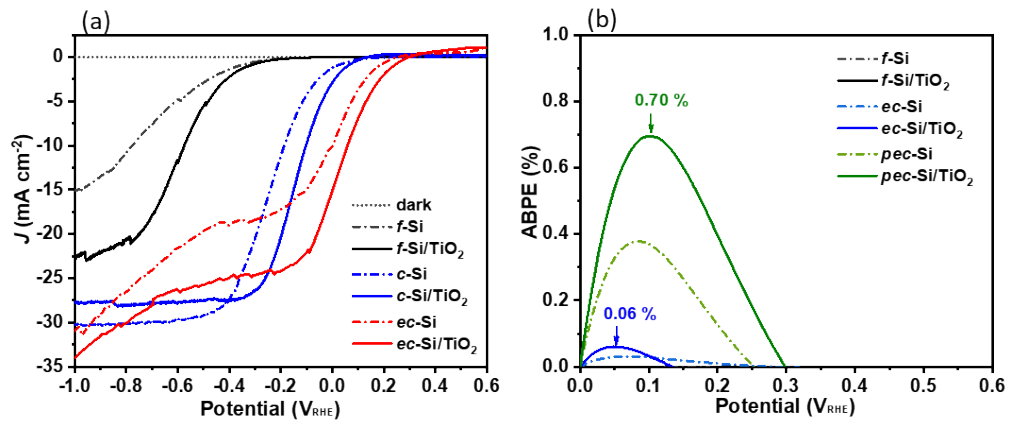


Figure S7. J - V curves (a) and ABPE (b) of TiO_2 -coated f -Si, c -Si and ec -Si photocathodes in 0.5 M H_2SO_4 under AM1.5G illumination.

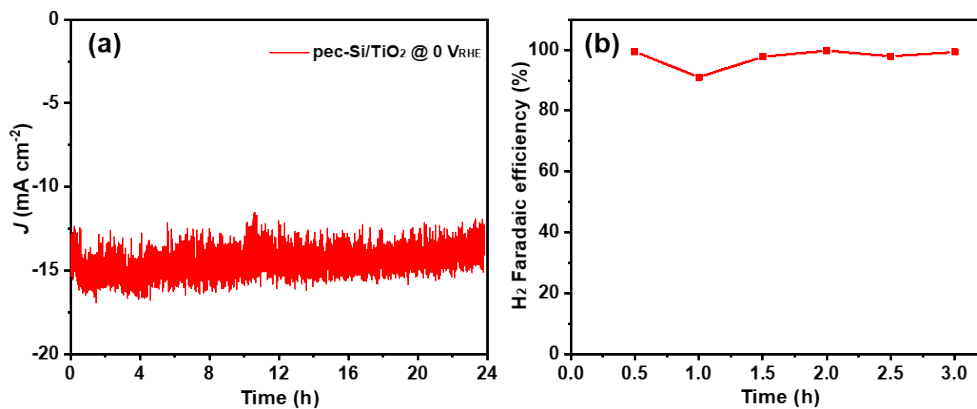


Figure S8. (a) $J-t$ curve of pec -Si/TiO₂ photocathode in 0.5 M H₂SO₄ at 0 V_{RHE} under the illumination of AM1.5G for over 24 h. (b) the H₂ evolution Faradaic efficiency of pec -Si/TiO₂ photocathode at 0 V_{RHE} is obtained from the gas chromatograph measurements, which is referring to the electrolysis of water by two Pt electrodes (assumed to be 100% for H₂ production) in the same electrolyte with a similar current density.

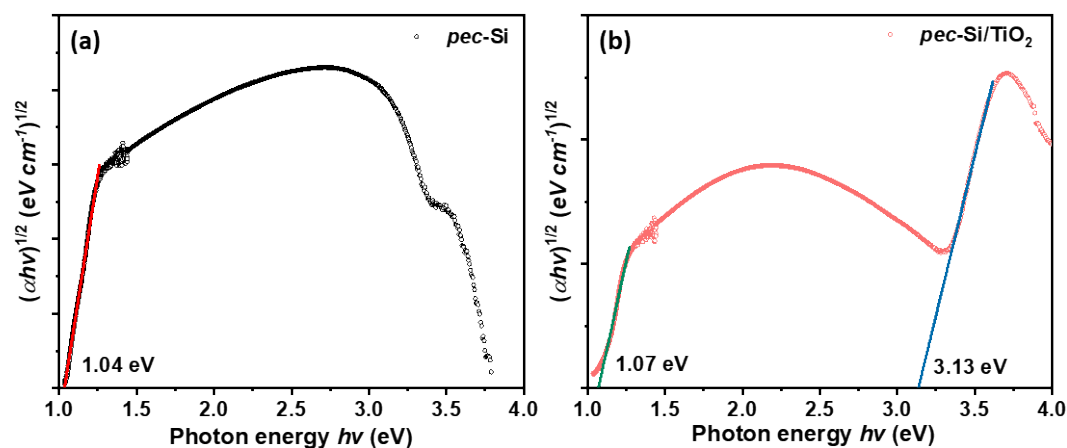


Figure S9. Tauc plots of pec -Si (a) and pec -Si/TiO₂ (b), illustrating the bandgaps of Si (1.07 eV) and TiO₂ (3.13 eV).

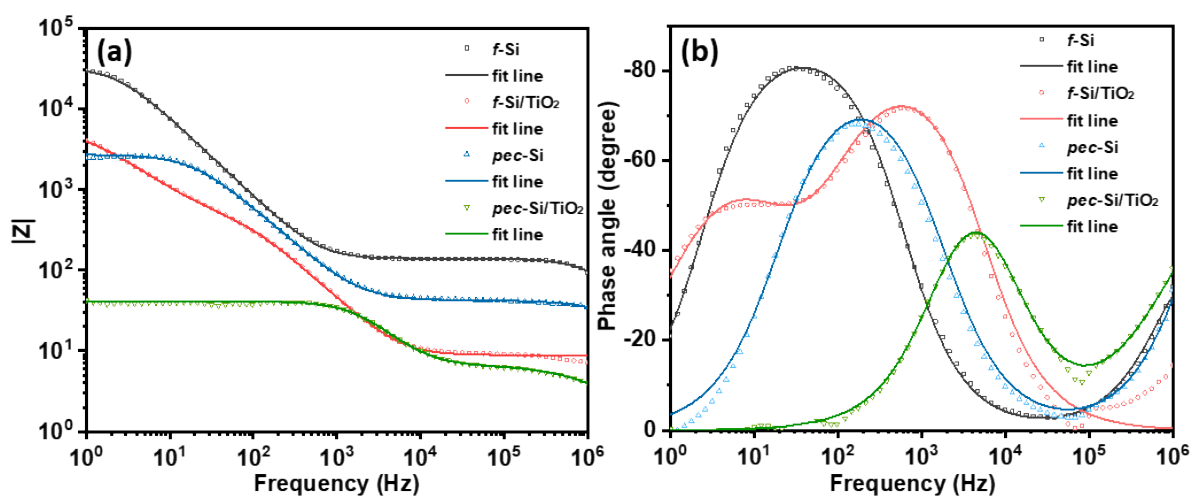


Figure S10. Bode impedance (a) and Bode phase (b) plots of f -Si, f -Si/TiO₂, pec -Si and pec -Si/TiO₂.

Table S1. A comparison of the J_{ph} at 0 V_{RHE} and E_{on} of the nanostructured Si photocathodes for PEC water splitting reported recently.

N o.	Si Photocathode	Fabrication of Si electrode	PEC conditions	J_{ph} at 0 V_{RHE} (mA cm ⁻²)	E_{on} (V_{RHE})	Ref.
1	Polished Si	--	0.5 M H ₂ SO ₄	0	-0.17	<i>Energy Environ. Sci.</i> , 2011 , 4, 1690. ¹
	Nanoporous Si	Chemical-etching (HAuCl ₄ + H ₂ O ₂)		0	-0.10	
2	Planar p-Si	--	1 M HClO ₄ ; $\lambda > 620$ nm	0	-0.4	<i>Nat. Mater.</i> , 2011 , 10, 434. ²
	Pillar p-Si	UV-lithography		-1.0	+0.05	
	Pillar p-Si/[Mo ₃ S ₄]			-8.0	+0.15	
3	Planar p-Si/MoS ₂	--	0.5 M H ₂ SO ₄ ; AM1.5G	-10.0	+0.23	<i>J. Mater. Chem. A</i> , 2017 , 5, 3304. ³
4	Pyramid p-Si/TiO ₂ /CoS _x	Chemical-etching (KOH)	0.5 M H ₂ SO ₄ ; AM1.5G	-20.6	+0.14	<i>ACS Appl. Mater. Interfaces</i> , 2018 , 10, 37142. ⁴
5	Planar p-Si	--	0.5 M H ₂ SO ₄ ; AM1.5G	-0.39	+0.06	<i>ACS Appl. Mater. Interfaces</i> , 2018 , 10, 23074. ⁵
	Planar p-Si/ReS ₂			-9.0	+0.36	
6	p-Si/Ni(TEOA) ₂ Cl ₂	--	0.5M H ₂ SO ₄ ; AM1.5G	-5.57	+0.11	<i>Appl. Catal. B</i> , 2018 , 220, 362. ⁶
	p-Si/Pt			-10	+0.19	
7	p-Si	--	0.2 M H ₂ SO ₄ ; AM1.5G	-0.5	+0.11	<i>Energy Environ. Sci.</i> , 2019 , 12, 1088. ⁷
	p-Si/Pt	Chemical-etching (HF + H ₂ O ₂ + AgNO ₃)		-9.2	+0.38	
	p-Si/MoS _x			-19.5	+0.38	
8	Pyramid p-Si/TiO ₂ /MoS ₂	Chemical-etching (KOH)	0.5 M H ₂ SO ₄ ; AM1.5G	-0.24	+0.42	<i>ACS Appl. Energy Mater.</i> , 2020 , 4, 730. ⁸
9	Pyramid p-Si/TiO ₂ /PO-WMoS	Chemical-etching (KOH)	0.5 M H ₂ SO ₄ ; AM1.5G	-15.0	+0.246	<i>ACS Appl. Mater. Interfaces</i> , 2020 , 12, 41515. ⁹
10	Pyramid p-Si/CoS ₂	Chemical-etching (Cu ²⁺ + HF + H ₂ O ₂)	0.05 M H ₂ SO ₄ ; AM1.5G	-6.60	+0.22	<i>Nanoscale</i> , 2020 , 12, 316. ¹⁰
11	Nanoporous p-Si	Chemical-etching (KOH + H ₂ O ₂)	0.5 M H ₂ SO ₄ ; AM1.5G	-8	+0.229	<i>Adv. Funct. Mater.</i> , 2021 , 31, 2008888. ¹¹
	Nanoporous p-Si/Pt			-15	+0.229	
12	c-Si	Chemical-etching (KOH)	0.5 M H ₂ SO ₄ ; AM1.5G	-1.2	+0.30	This work
	ec-Si	Electrochemical-etching (HF)		-10.1	+0.26	
	pec-Si	Photoelectrochemical-etching (HF)		-16.8	+0.42	
	pec-Si/TiO ₂			-15.5	+0.60	

Table S2. Fitting results of the EIS data for *f*-Si, *f*-Si/TiO₂, *pec*-Si and *pec*-Si/TiO₂ photoanodes.

Electrodes	R _s (Ω·cm ²)	R _{bulk} (Ω·cm ²)	R _{ct} (Ω·cm ²)	CPE _{ct-T}	CPE _{ct-P}	CPE _{cs-T}	CPE _{cs-P}
f-Si	36.7	102.5	31728	2.2 × 10 ⁻⁶	0.98	2.6 × 10 ⁻⁹	0.97
f-Si/TiO₂	8.8	604.8	5678	3.6 × 10 ⁻⁵	0.79	5.6 × 10 ⁻⁶	0.95
pec-Si	0.10	42.3	2678	4.3 × 10 ⁻⁶	0.92	7.4 × 10 ⁻⁹	0.92
pec-Si/TiO₂	0.07	6.8	34.3	3.8 × 10 ⁻⁶	0.96	1.1 × 10 ⁻⁶	0.76

Reference:

1. J. Oh, T. G. Deutsch, H.-C. Yuan and H. M. Branz, *Energy Environ. Sci.*, 2011, **4**, 1690-1694.
2. Y. Hou, B. L. Abrams, P. C. Vesborg, M. E. Bjorketun, K. Herbst, L. Bech, A. M. Setti, C. D. Damsgaard, T. Pedersen, O. Hansen, J. Rossmeisl, S. Dahl, J. K. Nørskov and I. Chorkendorff, *Nat. Mater.*, 2011, **10**, 434-438.
3. S. Oh, J. B. Kim, J. T. Song, J. Oh and S.-H. Kim, *J. Mater. Chem. A*, 2017, **5**, 3304-3310.
4. C. J. Chen, C. W. Liu, K. C. Yang, L. C. Yin, D. H. Wei, S. F. Hu and R. S. Liu, *ACS Appl. Mater. Interfaces*, 2018, **10**, 37142-37149.
5. H. Zhao, Z. Dai, X. Xu, J. Pan and J. Hu, *ACS Appl. Mater. Interfaces*, 2018, **10**, 23074-23080.
6. W. Zhou, F. Niu, S. S. Mao and S. Shen, *Appl. Catal. B*, 2018, **220**, 362-366.
7. L. Lu, W. Vakki, J. A. Aguiar, C. Xiao, K. Hurst, M. Fairchild, X. Chen, F. Yang, J. Gu and Z. J. Ren, *Energy Environ. Sci.*, 2019, **12**, 1088-1099.
8. X. Li, Y. Li, H. Wang, H. Miao, H. Zhu, X. Liu, H. Lin and G. Shi, *ACS Appl. Energy Mater.*, 2020, **4**, 730-736.
9. K. Pichaimuthu, C. J. Chen, C. H. Chen, Y. T. Chen, C. Su, D. H. Wei and R. S. Liu, *ACS Appl. Mater. Interfaces*, 2020, **12**, 41515-41526.
10. S. Zhao, G. Yuan, Q. Wang, W. Liu, R. Wang and S. Yang, *Nanoscale*, 2020, **12**, 316-325.
11. M. Patrick, F. Yang, W. Vakki, J. A. Aguiar and J. Gu, *Adv. Funct. Mater.*, 2021, **31**, 2008888.